

State-to-state dynamics in the high Rydberg states of polyatomic molecules

E. Mayer, E. Zückerman, L. Zhang, H. Hedderich, J. Behm and E. R. Grant

Phil. Trans. R. Soc. Lond. A 1997 **355**, 1569-1583

doi: 10.1098/rsta.1997.0077

Email alerting service

Receive free email alerts when new articles cite this article - sign up in the box at the top right-hand corner of the article or click [here](#)

To subscribe to *Phil. Trans. R. Soc. Lond. A* go to: <http://rsta.royalsocietypublishing.org/subscriptions>

State-to-state dynamics in the high Rydberg states of polyatomic molecules

BY E. MAYER, E. ZÜCKERMAN, L. ZHANG, H. HEDDERICH,
J. BEHM AND E. R. GRANT

Department of Chemistry, Purdue University, West Lafayette, IN 47907, USA

Rydberg states in polyatomic molecules exhibit dynamics that bear on issues of longstanding importance for theory. Coupling is made complicated, however, by the presence of many rovibrational degrees of freedom and the existence of multiple pathways for intramolecular relaxation. In work on vibrationally autoionizing states of HCO and NO₂, we have applied multiple resonance excitation strategies to isolate single rovibrational Rydberg–Rydberg transitions, the positions, lineshapes and intensities of which reflect coupling strengths for state-detailed relaxation processes.

1. Introduction

The effort to describe energy flow in isolated molecules has served for many years as an important focus of research in chemical physics (see, for instance, McDonald 1979; Jortner & Levine 1981; Smalley 1983). Work in this field has added a great deal to our understanding of chemical reactivity and remains today as a vital point of contact between experimental and theoretical studies in molecular dynamics (Crim 1993; Schinke *et al.* 1995; Dai & Field 1995). A particularly important pathway for intramolecular relaxation is the transfer of energy between electronic and internuclear degrees of freedom. Details in the dynamics of radiationless decay can give rise to significant chemical consequences and factors regulating the magnitudes of non-Born–Oppenheimer coupling terms underlie contemporary efforts to externally control paths of intramolecular relaxation and direct the outcomes of chemical reactions (Shapiro & Brumer 1994; Warren *et al.* 1993; Kohler *et al.* 1995).

Electronic relaxation pathways that exist in molecular Rydberg states offer a particularly well-defined set of model non-Born–Oppenheimer processes (Jortner & Leach 1980). Here, the dynamics of intramolecular energy transfer that lead to electron ejection can be conveniently framed in terms of coupling between well-defined approximately separable orbital–electronic and cation–core internal degrees of freedom (Fano 1983; Greene & Jungen 1985). These dynamics are important because they are universal. All substances can be ionized and, in the elementary properties of electron ejection, the process of intramolecular relaxation finds common expression in a very broad class of systems. Photoionization and particularly autoionization are well-defined forms of state-to-state fragmentation. Specific interactions encountered in this regime are relevant to the elementary dynamics of electron transfer (Fox 1992) and connect directly with theories of electron–cation inelastic scattering (Greene & Jungen 1985; Lucchese *et al.* 1986; Ross 1991). In practice, multiresonant excitation schemes can exploit the separability of excited electronic degrees of freedom near

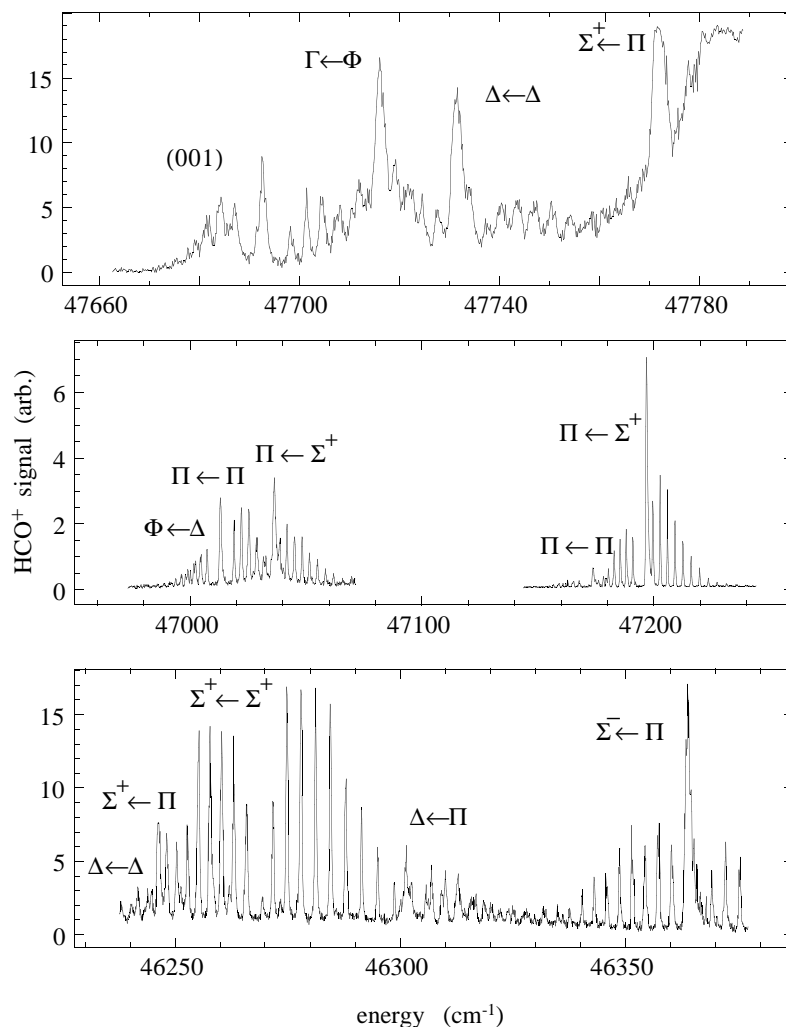


Figure 1. $(1+1)$ resonant ionization spectra of HCO with assignment of transitions to vibronic components split by Renner–Teller effects in $3p\pi$ vibrational levels (010) and (020) with a portion of (030) showing the spectrum of the interloping (001) CO stretch band. Lower-state symmetry designations refer to originating values of the rotational angular momentum quantum number K in these bent-to-linear transitions.

the ionization threshold to achieve photoselection (Grant 1988; Schlag *et al.* 1995). Some measure of selectivity has already been achieved and photoionization is the first process for which coherent optical control has been demonstrated (Chen *et al.* 1990, Chen & Elliott 1990; Park *et al.* 1991; Yin *et al.* 1992, 1995; Kleinman *et al.* 1995).

In the present work we examine the transfer of energy between vibrational and Rydberg electronic degrees of freedom in small polyatomic molecules, with a particular focus on the mode dependence of relaxation leading to electron ejection (vibrational autoionization). The principal systems of interest are NO_2 and HCO, both of which possess Rydberg states built on linear closed-shell cation cores. We report on the intramolecular decay dynamics of high Rydberg states which are vibrationally excited in isolated fundamentals, as well as in higher levels where anharmonic coupling be-

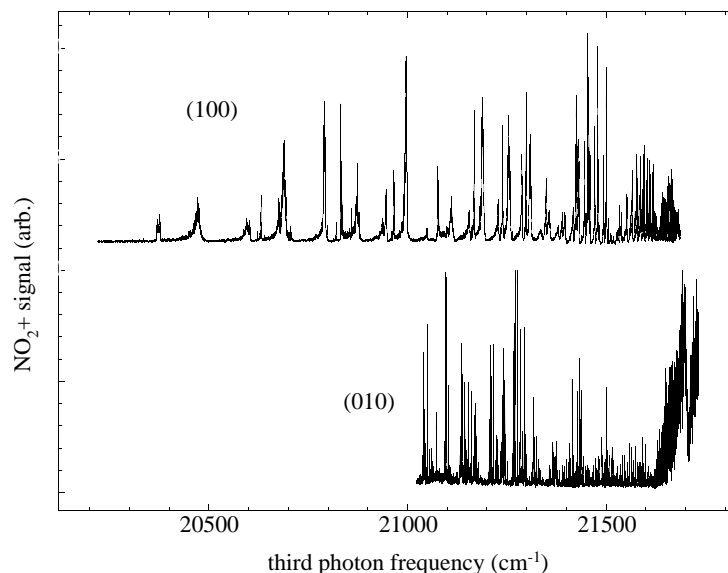


Figure 2. Vibrational autoionization spectrum of NO_2 Rydberg series built on symmetric stretch (100) and bending (010) vibrationally excited states of the core.

tween normal modes in the core affects vibrational-Rydberg relaxation. Our results for these two systems form consistent patterns that suggest mode-dependent trends in the dynamics of vibrational autoionization and illuminate broader issues connected with the control of vibrationally mediated fragmentation processes in general.

2. Experimental method

We prepare autoionizing states of NO_2 in a sequence of three resonant transitions starting from the bent 2A_1 ground state to discrete levels of the vibronically active 2B_2 state, then to gateway rovibrational levels of the linear $3p\sigma\ {}^2\Sigma_u^+$ Rydberg state and then, finally, to high Rydberg series converging to like vibrational states of the cation (Campos *et al.* 1990*a,b*, 1991; Bryant *et al.* 1992*a*; Matsui & Grant 1996). In separate experiments, single-colour $(2 + 1)$ resonance enhanced multiphoton ionization spectroscopy provides a broader survey of rovibrational structure in the $3p\sigma\ {}^2\Sigma_u^+$ Rydberg state of this molecule (Matsui *et al.* 1996). We excite the HCO radical in two steps starting with a one-photon transition from the bent ${}^2A'$ ground state to single rovibrational levels of the linear $3p\pi\ {}^2\Pi$ Rydberg state. Photoselected levels in this gateway Rydberg state then serve as originating levels for vertical scans over vibrational autoionizing intervals (Mayer & Grant 1995).

NO_2 , seeded 1:1:20 in $\text{O}_2:\text{He}$, is cooled by expansion through a pulsed molecular beam valve (General Valve, IOTA 1). A jet of HCO is produced in similar fashion by photolysis of acetaldehyde at the exit of the valve. In both cases the jet passes through a differential wall into a chamber housing an Extranuclear quadrupole mass spectrometer.

Tunable radiation is provided by Lambda-Physik excimer- and Continuum Nd:YAG-pumped dye lasers in various combinations. Frequency doubling in beta-barium borate (BBO) produces ultraviolet radiation where required. The excimer and YAG lasers run at 10 Hz. Dye-laser bandwidths are *ca.* $0.2\ \text{cm}^{-1}$.

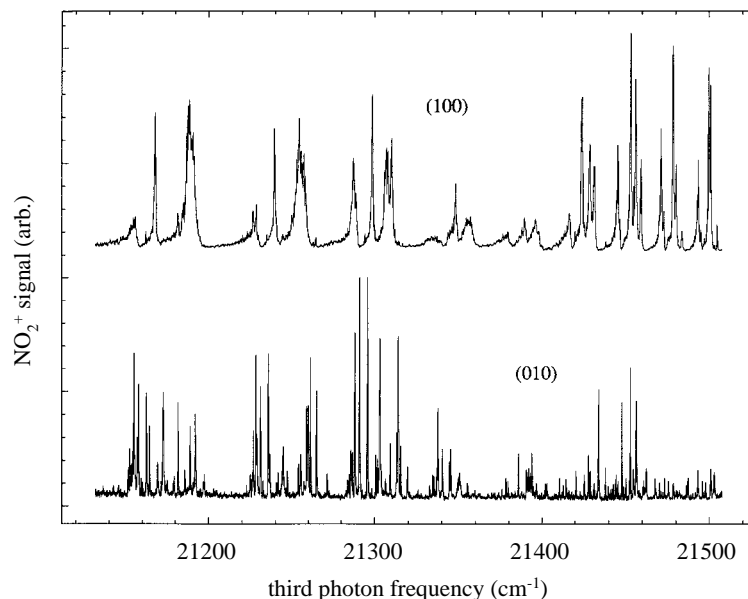


Figure 3. A detailed view of vibrational autoionization linewidths for series with principal quantum number from $n = 14$ to 22 converging to symmetric stretch and bending excited states of NO_2^+ .

Ions produced by vibrational autoionization are mass filtered and detected by a Galileo channeltron electron multiplier. The output of the detector is amplified and collected by a LeCroy 9450 digital oscilloscope which is read by a laboratory computer. Wavelengths of the dye lasers are calibrated by a Burleigh W-4500 pulsed wavemeter.

3. Results

(a) Gateway Rydberg states

The $(2 + 1)$ resonance-enhanced multiphoton ionization spectrum of the $3p\sigma^2\Sigma_u^+$ Rydberg state of NO_2 shows a long progression of vibrational levels consisting of fundamentals, overtones and combinations of symmetric stretch, asymmetric stretch and bend (Matsui *et al.* 1996). Relative positions assigned to these levels match closely with vibrational frequencies determined for the cation itself by ZEKE high-resolution threshold photoionization spectroscopy (Bryant *et al.* 1992b). In both the cation and the $3p\sigma$ Rydberg state, moderate Fermi resonance couples overtone and combination states of the bend with levels of symmetric stretch. Analysis yields anharmonic coupling terms comparable to those of neutral CO_2 . Perturbations here are smaller, however, because the harmonic frequency for symmetric stretch in NO_2^+ differs more from that of its bending overtone.

With still greater bend-stretch frequency separations, and thus little possibility for Fermi resonance, the low-lying vibrational states of HCO^+ factor as approximately separable harmonic oscillators (Amano 1981; Foster *et al.* 1981; Davies *et al.* 1984; Davies & Rothwell 1984). In the $\text{HCO } 3p\pi^2\Pi$ Rydberg state, however, Renner–Teller coupling mixes vibrational angular momentum components and produces observable perturbations in vibronic positions (Song & Cool 1992; Mayer *et al.* 1997).

Table 1 summarizes vibrational frequencies in the $3p\sigma^2\Sigma_u^+$ state of NO_2 and the

Table 1. Vibrational frequencies in the $3p\sigma^2\Sigma_u^+$ state of NO_2 and the $3p\pi^2\Pi$ state of HCO , compared with fundamental frequencies for the corresponding cations

	NO_2		HCO	
	$3p\sigma^2\Sigma_u^+$ Rydberg state	$X^1\Sigma_u^+$ cation	$3p\pi^2\Pi$ Rydberg state	$X^1\Sigma^+$ cation
(010)	621	627	800 ^b	830
(020)	1238 ^a	1234 ^a	1600 ^b	1687
(100)	1401	1387		3089
(001)	2361	2362	2217	2184

^aObserved frequency of (02⁰0).

^bHarmonic bending frequencies (deperturbed).

$3p\pi^2\Pi$ state of HCO , compared with fundamental frequencies established for the corresponding cations. Table 2 lists the bend-stretch harmonic separation together with Fermi resonance coupling parameters for NO_2 and Renner–Teller constant for HCO . Figure 1 shows typical (1 + 1) resonant ionization spectra of HCO with assignment of Renner–Teller components in $3p\pi$ vibrational levels (010) and (020), as well as a detail of the (030) complex exhibiting the interloping (001) band. Complete assignment of these spectra with an analysis characterizing Renner–Teller and Fermi-resonance effects will appear in a forthcoming paper (Mayer *et al.* 1997). The NO_2 results have been published in full (Matsui *et al.* 1996).

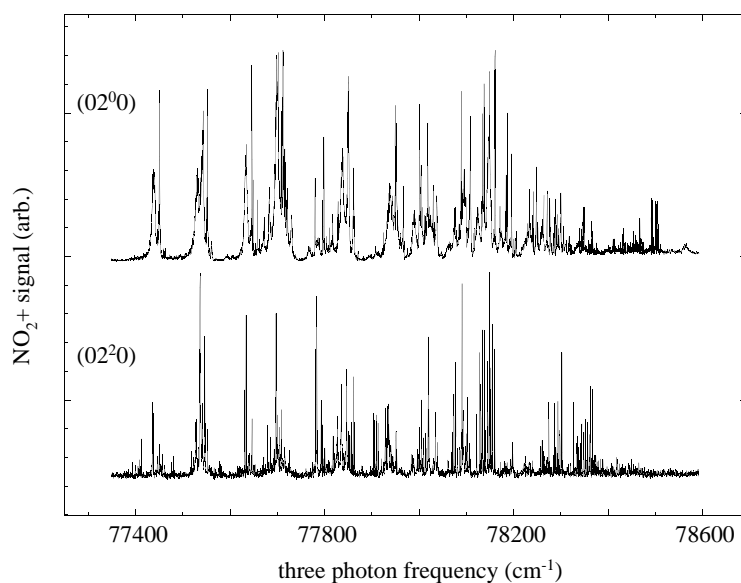
(b) High-Rydberg states and autoionization dynamics

Individual rotational levels selected in $n = 3$ Rydberg vibrational bands of NO_2 and HCO serve as starting points for vertical transitions to series of autoionizing Rydberg states. Figure 2 shows scans over (100) and (010) autoionizing intervals for NO_2 . Figure 3 gives a detailed view comparing linewidths for transitions to autoionizing principal quantum numbers $n = 14$ –22. In these spectra, transitions originating in the $3p\sigma^2\Sigma_u^+$ state reach series labelled in Hund's case (b) as $s\sigma$, $d\sigma$ and $d\pi$ converging to corresponding vibrational states of the cation. Governed by the same electronic selection rules, figure 4 shows resonances that decay by relaxation of core overtone components, (02⁰0) and (02²0). In these spectra, we find linewidths comparable to (100) for (02⁰0), while (02²0) linewidths more resemble those found for (010). For both overtone systems in NO_2 , we observe that intensities remain uniform over the full range, including Rydberg electronic energies for which autoionization requires $\Delta v = -1$ as well as lower values of n where relaxation of both quanta of bend is needed for electron ejection.

Figures 5–7 show comparable survey autoionization spectra for HCO . Figure 4 compares structure built on cores in excited states, (001) and (010) over their full autoionization intervals. Figure 6 details lineshapes for principal quantum numbers $n = 12$ –16. Figure 7 shows the autoionization spectrum for HCO prepared by photoselection of a single rotational line in the isolated upper Π component of the first overtone of the bend in the $3p\pi$ state (cf. figure 1). Note the break in the apparent intensities (ion yields) which can be seen in the (020) autoionization spectrum at the threshold for autoionization by $\Delta v = -1$.

Table 2. Fermi resonance coupling parameters for NO_2^+ and Renner–Teller constant for HCO (all parameters in cm^{-1})

	harmonic spacing Δ_0	Fermi resonance matrix element $W_{(100)-(020)}$	cubic anharmonicity k_{122}
$\text{NO}_2^+ X^1\Sigma_u^+$	122	45.7	−64.6
Renner–Teller coupling constant			
HCO $3p\pi^2\Pi$		$0.07 \omega_2$	

Figure 4. Autoionizing resonances in NO_2 that decay by the relaxation of bending overtone components (02^0) and (02^2) .

4. Discussion

(a) Originating states for Rydberg–Rydberg transitions

Transitions to autoionizing series in NO_2 and HCO originate from photoselected levels in intermediate states which are affected to varying degrees by vibrational and vibronic coupling. In NO_2 , Fermi resonance mixes symmetric stretch with symmetric overtones of the bend. From coupling coefficients, we estimate a 12% mixture of symmetric stretch in (02^0) (Matsui *et al.* 1996). Though not sufficient to appear in the rotational simulations that we use to establish vibrational positions, some degree of Coriolis coupling can be expected to mix (02^2) with (02^0) (Bolman *et al.* 1975).

In HCO, cation–core Fermi resonance is weak, but the vibrational angular momentum components of excited bending levels in the originating state are substantially mixed by Renner–Teller coupling with the $3p\pi$ Rydberg electron. Because this electronic orbital angular momentum involves motion which is relatively distant from

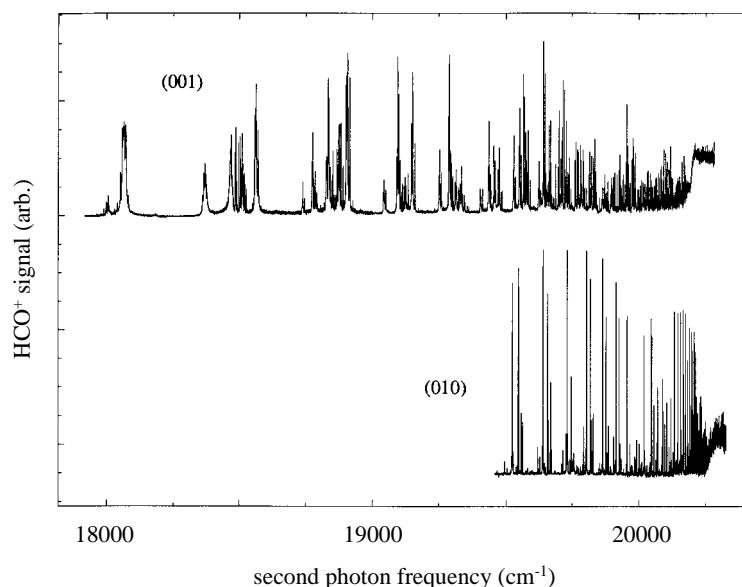


Figure 5. Vibrational autoionization spectrum of HCO Rydberg series built on CO stretch (001) and bending (010) vibrationally excited states of the core.

the core, coupling is smaller than that typically found in valence Π states. Nevertheless, vibronic coupling is sufficient to produce distinctly separated bands at the (020) level and yield Franck–Condon transition intensity from either Π component of the Rydberg intermediate state to very weakly split (020) ion–core vibrational levels characterized by vibrational $l = 0$ and 2 (Hougen 1962).

(b) *Core vibrational coupling and mode selectivity in autoionization linewidths*

Autoionization linewidths for NO_2 show a clear distinction between the relaxation of symmetric stretch and bending fundamentals. Stretching resonances appear uniformly much broader than those built on the bend. To account for this difference, it is natural to look to differences in symmetry and effects due to angular momentum constraints on relaxation from symmetric stretch and bend.

The transfer of energy from τ_g symmetric stretch excited states to the Rydberg electron occurs as in a diatomic molecule, without the need for exchange of core and Rydberg electronic angular momentum. Thus, broad linewidths in stretching series, particularly for penetrating, larger quantum defect orbitals, might simply reflect the straightforward way in which the symmetric stretching vibration couples bound ns and nd Rydberg states to the totally symmetric vibrationless continuum.

The symmetry and angular momentum requirements for decay of bending excited states are more complex. In particular, the presence of vibrational angular momentum uniquely distinguishes linear triatomics from diatomic molecules. In NO_2 , to conserve symmetry and obey nuclear spin statistics, energy transfer from a vibrationally π_u (010) bending level to the continuum of the totally symmetric vibrationless (000) core must be accompanied by a change in leaving-electron angular momentum (and core rotational state in some cases). Sharp linewidths show that this process proceeds much more slowly.

At the overtone of the bend, high-Rydberg resonances built on the totally symmetric (02⁰0) bending overtone state of the core decay much faster than those of

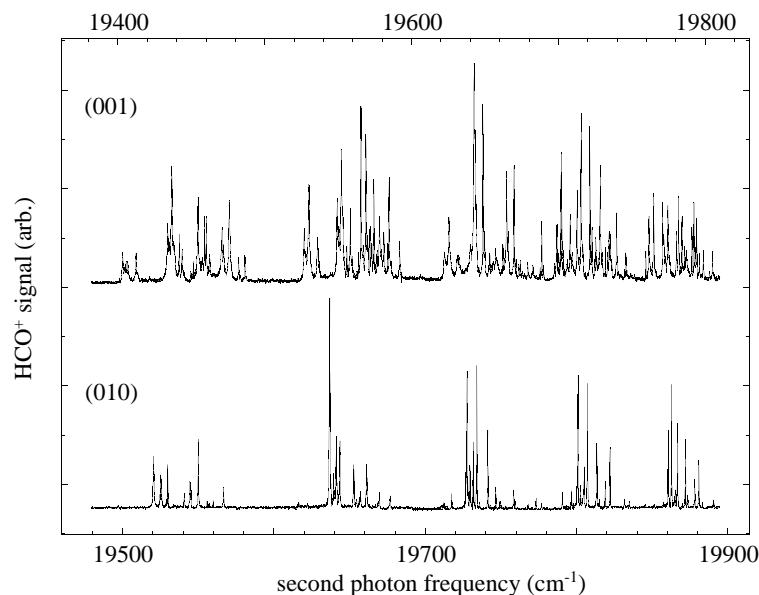


Figure 6. A detailed view of vibrational autoionization linewidths for series with principal quantum number from $n = 12$ to 16 converging to CO stretch and bending excited states of HCO^+ .

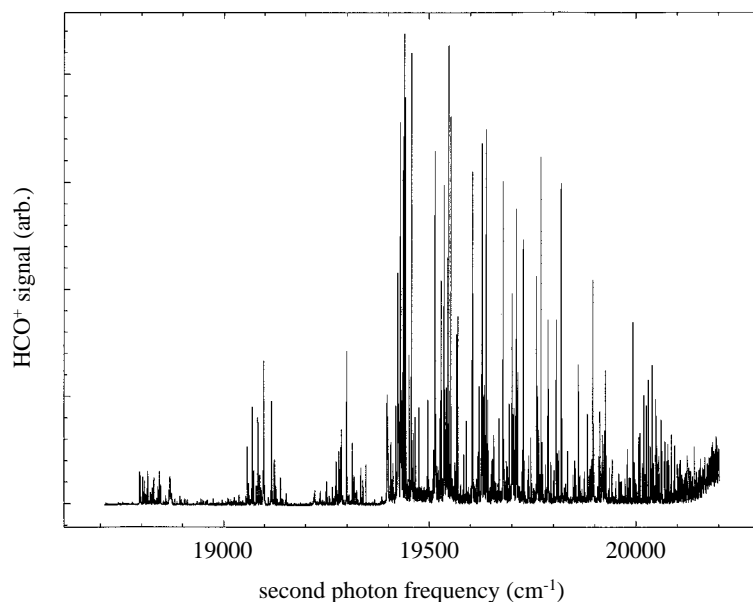


Figure 7. Autoionizing resonances in HCO^+ that decay by the relaxation of the bending overtone (020) (includes components with vibrational angular momentum designations (02^0_0) and (02^2_0)).

the fundamental, with rates, judging from linewidths, that compare with decays driven by relaxation of symmetric stretch. Series built on the higher angular momentum, (02^2_0) state are sharper, exhibiting linewidths similar to those found for the (010) bending fundamental. For both vibrational angular momentum states of the core, (020) autoionization intensities remain constant and linewidths scale con-

sistently over the full two-quantum interval. This is surprising, because vibrational autoionization often exhibits a propensity that favours autoionization by $\Delta v = -1$. Consistency in the intensities of resonances for both $\Delta v = -1$ and -2 suggests that a uniform mechanism operates to drive (020) autoionization throughout the region from the adiabatic threshold to the vertical limit.

Splittings apparent in the vibrational structure of the NO_2^+ cation establish that Fermi resonance mixes symmetric stretch with the symmetric overtone of the bend and, though not explicitly observed, Coriolis terms can be expected to couple (02⁰⁰) with (02²⁰). The component of (020) autoionization driven by mixing with (100) will be present over the full interval between the (000) and (100) thresholds, which spans that of (020). Both (02⁰⁰) and (02²⁰) states of the core can be expected to acquire (100) character, (02⁰⁰) by Fermi resonance with (100), and (02²⁰) by Coriolis coupling with (02⁰⁰). Uniform intensities of autoionization resonances over an energy interval formally requiring $\Delta v_2 = -1$ and -2 signal the role of (100) in promoting electron loss and linewidths appear to scale qualitatively with the degree of mixing. Thus, it appears from the data that the extent of stretching character is more important than symmetry per se in determining the autoionization lifetimes of (02⁰⁰) and (02²⁰).

Results for HCO tend to confirm this conclusion. Again for fundamental vibrations, autoionization driven by relaxation of the CO stretching vibration is faster than decay of the HCO bend. At the overtone of the bend, for this case in which Fermi resonance is not important, series converging to (020), which include both $l = 0$ and 2 (σ and δ) vibrational angular momentum components of the core—mixed in the originating state and infinitesimally split in the high-Rydberg core—are uniformly sharp and exhibit a substantial drop at $\Delta v = -1$ threshold. We suggest that HCO behaves differently (showing normal $\Delta v = -1$ propensity) because Fermi resonance is absent and the totally symmetric (02⁰⁰) state of HCO^+ has little stretching character. Thus, comparing HCO with NO_2 , lifetimes in the overtone again appear to correlate more with degree of stretch than symmetry.

From these observations on NO_2 and HCO, we can recognize vibrational autoionization as a vibrationally mediated photofragmentation process with a high degree of mode specificity. Selecting the mode of vibration, we control the rate of fragmentation. In HCO, for which vibrational coupling is weak, control extends to the overtone of the bend. In NO_2 , however, Fermi resonance mixes stretch with bend to a small but significant degree, and all specificity is lost in the symmetric overtone of the bend. In this way, autoionization provides a clear-cut demonstration of the limitations that can be imposed by intramolecular relaxation on the specificity of control by vibrational mediation.

(c) *Vibrational autoionization dynamics*

What is the mechanism by which selection of normal mode regulates the rate of autoionization? The resonances that appear in the spectra presented in figures 2–7 reflect the coupling of vibrationally excited closed-channel Rydberg states with open channels built on the ground state and lower-lying excited vibrational levels of NO_2^+ and HCO^+ cation cores. Coupling of this kind is well described formally in the language of multichannel quantum defect theory (MQDT). Intramolecular relaxation redistributes energy and angular momentum among vibration, rotation and Rydberg electronic degrees of freedom. MQDT factors this process into two distinct coupling regimes, one referenced to the body frame, which applies when

the electron is close to the core, and the other referenced to the laboratory frame when it is far away. Scattering interactions that transfer angular momentum between the Rydberg electronic and molecular vibrational and rotational degrees of freedom occur when the electron is coupled to the body frame. A transformation of frame projects these short-range interactions to determine the energetics and dynamics of high Rydberg states (see, for example, Greene & Jungen 1985; Ross 1991, Ross & Jungen 1994).

MQDT is particularly well developed in its application to the vibrational autoionization of diatomic molecules. The theory formed in the pioneering work of Jungen with Atabek (1977), Dill (1980) and Raoult (1981), specifically describes resonances in terms of asymptotic channel functions constructed from a long-range Coulomb basis, coupled by a rovibronic reaction matrix,

$$K_{iv_i^+ N_i^+, jv_j^+ N_j^+},$$

where N^+ refers to cation angular momentum and v_i is the quantum number of the single vibrational degree of freedom. Physically, these channel wavefunctions correspond to scattering states in which an electron with angular momentum l_i collides with a cation in electronic vibrational-rotational state $|iv_i^+ N_i^+\rangle^{\text{JM}}$ to produce a final state which is a mixture of all accessible channels, $e_j > |jv_j^+ N_j^+\rangle^{\text{JM}}$.

Close to the core, the fast-moving electron samples a single internuclear separation in undergoing interactions which are largely independent of its asymptotic energy. The appropriate basis in this collision-channel region is comprized of the Born-Oppenheimer products of electronic functions, i , with core vibrational wavefunctions, written $|iRA\rangle^{\text{JM}}$, where i represents a generalized electronic quantum number, R is the internuclear distance and A is the well defined projection of the total orbital angular momentum on the internuclear axis.

Close-coupled scattering states are mixed by the R -dependent electronic $K^A(R)$ matrix, which follows directly from the electronic or eigenchannel quantum defect matrix, $\mu^A(R)$. As noted above, a rovibrational frame transformation projects collision-channel interactions on the manifold of asymptotic states to define the full rovibronic K matrix:

$$K_{iv_i^+ N_i^+, jv_j^+ N_j^+} = \int dR^{\text{JM}} \left\langle iv_i^+ N_i^+ \left| \left\{ \sum_{sLa} |iRA\rangle^{\text{JM}} K_{ij}^A(R)^{\text{JM}} \langle jRA| \right\} \right| jv_j^+ N_j^+ \right\rangle^{\text{JM}},$$

where

$$K_{ij}^A(R) = \tan \pi \mu_{ij}^A(R).$$

In practice, the internuclear coordinate dependent eigenchannel quantum defect matrix, $\mu^A(R)$, is obtained from fits to experimental results, or from comparing *ab initio* potentials of the close-coupled Rydberg states with that of the cation.

Autoionization lineshapes arise from the accumulation of continuum phase about channel function eigenstates. Channel coupling matrix elements determine interaction widths. The magnitudes of these integrals depend on the R -dependence of $\mu^A(R)$. In practice, the quantum defect matrix can be approximated by an expansion about R_e and, for final vibrational states differing from initial ones by a single quantum, one finds vibrational autoionization matrix elements dominated by first-order terms. Orbital angular momentum and its projection can also be important. In H_2 , for example, μ_Σ varies strongly with R , while μ_Π is nearly constant. As a result, the autoionization is carried by σ - σ interactions, with interloping π resonances present only

to the extent that rotational l coupling mixes these channels (Herzberg & Jungen 1972; Raoult & Jungen 1981; Jungen & Raoult 1981).

In polyatomic molecules, the presence of more than one vibrational dimension adds degrees of freedom to the quantum defect matrix, while at the same time details associated with vibrational symmetry and angular momentum supply constraints and enable one to consider issues of vibrational as well as orbital shape. Theoretical work detailing the autoionization dynamics of polyatomics is early in its development. Bordas & Helm (1991) have applied MQDT to account for effects of l -uncoupling and rotational autoionization on positions and intensities in H_3 and Child & Jungen (1990) have extended diatomic MQDT in a rigid rotor approximation to vibrationally autoionizing high Rydberg states of H_2O . Although evident in the experimental data, neither of these studies included vibrational coupling. More recently, Stephens & Greene (1995) considered vibrational autoionization from degenerate Rydberg states of H_3 which proceeds via relaxation of the degenerate E' mode in a core with Jahn–Teller distortion induced by the Rydberg electron.

A new study by Jungen & Pratt (1997) directly addresses the problem of the normal mode dependence of vibrational autoionization in linear triatomics. The key, as with diatomics, is in the vibrational amplitude dependence of the quantum defects. For example, the diagonal element $\mu_\Sigma(R)$ describes how the vibrational potential in the $\Lambda = 0$ eigenchannel differs from that of the cation. Our experiments on NO_2 prepare even ns and nd autoionizing Rydberg series. A finite variation in $\mu_\Sigma(R)$ with R_1 (symmetric stretch) scatters an even ns electron orbiting a (100) core into the (000) $l = 0$ continuum. However, such diagonal collision-channel interactions for relaxing the bending fundamental (010) to (000) are forbidden by symmetry. Instead, off-diagonal $\sigma_g\text{--}\pi_u$ or $\pi_g\text{--}\sigma_u$ electronic coupling is required to carry the vibrationally π_u excited bending mode to the σ_g core ground state, while necessarily scattering a σ_g or π_g electron to the π_u or σ_u continuum. The off-diagonal elements of the quantum defect matrix that drive this coupling describe configuration mixing in the close-coupled collision states which is manifested by intersections and avoided crossings in multidimensional Rydberg potential surfaces.

To construct a physical picture, Jungen & Pratt relate autoionization induced by non-totally symmetric vibrations to the dipole moment produced by motion along the non-totally symmetric coordinate. Building on this idea, it is possible to express the complete multipolar cation core charge distribution as a tensor series in normal coordinates, R_ν . The lowest-order, scalar moment is formed from the dot products, $R_1 \cdot R_1$, $R_2 \cdot R_2$ and $R_3 \cdot R_3$. Displacement in all normal modes is necessary to span this cation charge monopole. If it is of proper symmetry in the point group of the molecule, a variation in this charge distribution produced by vibrational motion can be expected to induce autoionization (Berry & Nielsen 1970). In effect, the pseudo-potentials offer a way to represent the vibrational coordinate dependence of the quantum defects. The derivative of the scalar moment with respect to the bending coordinate has the same symmetry as the off-diagonal quantum defect matrix element $\mu_{s\sigma_g\text{--}p\pi_u}$, which is appropriate to couple $l = 0, 2$ (010) Rydberg states to the $l = 1$ continuum of (000). Similarly, the derivative of the scalar moment of the charge distribution with respect to R_1 has the symmetry required to drive (100) to (000) while preserving even electronic angular momentum. On geometric grounds, we can expect the latter (stretching) terms to give rise to larger matrix elements. The behaviour of symmetric bending overtones in the presence and absence of Fermi resonance suggests for NO_2 and HCO at least that stretching character plays a sig-

nificant role in regulating triatomic autoionization. Whether this role is a general one, or that effects due to symmetry and molecule-specific properties of electronic structure alone best differentiate mode-to-mode autoionization rates in polyatomic molecules, remains to be tested by calculations and further systematic experiments, especially ones that include asymmetric bent triatomics.

This work was supported by the National Science Foundation and CNRS (NSF Grant numbers CHE-9307131, CHE-9632862 and INT-9216810). E.R.G. thanks Christian Jungen and Stephen Pratt for helpful discussions.

References

- Amano, T. 1981 The ν_1 fundamental band of HCO^+ by difference frequency laser spectroscopy. *J. Chem. Phys.* **79**, 3595.
- Berry, R. S. & Nielsen, S. E. 1970 Dynamic coupling phenomena in molecular excited states. I. general formulation and vibronic coupling in H_2 . *Phys. Rev. A* **1**, 383.
- Bolman, P. S. H., Brown, J. M., Carrington, A., Kopp, I. & Ramsay D. A. 1975 A Re-investigation of the $A^2\Sigma^+ - X^2\Pi_i$ band system of NCO. *Proc. R. Soc. Lond. A* **343**, 17.
- Bordas, M. C., Lembo, L. J. & Helm, H. 1991 Spectroscopy and multichannel quantum-defect theory analysis of the np Rydberg series of H_3 . *Phys. Rev. A* **44**, 1817.
- Brumer, P. & Shapiro, M. 1992 Laser control of molecular processes. *A. Rev. Phys. Chem.* **43**, 257.
- Bryant, G., Jiang, Y. & Grant, E. R. 1992a Triple-resonance spectroscopy of the higher excited states of NO_2 . IV. Trends in the mode dependence of vibrational autoionization via asymmetric stretch vs. symmetric stretch and bend. *J. Chem. Phys.* **96**, 4827.
- Bryant, G., Jiang, Y. & Grant, E. R. 1992b The vibrational structure of the NO_2 cation. *Chem. Phys. Lett.* **200**, 495.
- Campos, F. X., Jiang, Y. & Grant, E. R. 1990a Triple-resonance spectroscopy of the higher excited states of NO_2 : rovibronic interactions, autoionization and l -uncoupling in the (100) manifold. *J. Chem. Phys.* **93**, 2308.
- Campos, F. X., Jiang, Y. & Grant, E. R. 1990b Triple-resonance spectroscopy of the higher excited states of NO_2 . II. Vibrational mode selectivity in the competition between predissociation and autoionization. *J. Chem. Phys.* **93**, 7731.
- Campos, F. X., Jiang, Y. & Grant, E. R. 1991 Triple-resonance spectroscopy of the higher excited states of NO_2 . III. $|\Delta v| > 1$ autoionization and vibronic coupling. *J. Chem. Phys.* **94**, 5897.
- Chen, C., Yin, Y. & Elliott, D. S. 1990 Interference between optical transitions. *Phys. Rev. Lett.* **64**, 507.
- Chen, C. & Elliott, D. S. 1990 Measurements of optical phase variations using multiphoton ionization processes. *Phys. Rev. Lett.* **65**, 1737.
- Child, M. S. & Jungen, Ch. 1990 Quantum defect theory for asymmetric tops: Application to the Rydberg spectrum of H_2O . *J. Chem. Phys.* **93**, 7756.
- Cornaggia, C., Giusti-Suzor, A. & Jungen, Ch. 1987 Photoionization of the EF excited state of H_2 ; calculation of vibrational branching ratios and photoelectron angular distributions. *J. Chem. Phys.* **87**, 3934.
- Crim, F. F. 1993 Vibrationally mediated photodissociation. *A. Rev. Phys. Chem.* **44**, 397.
- Dai, H. L. & Field, R. W. (eds) 1995 *Molecular dynamics and spectroscopy by stimulated emission pumping*. Singapore: World Scientific.
- Davies, P. B., Hamilton, P. A. & Rothwell, W. J. 1984 Infrared laser spectroscopy of the ν_3 fundamental of HCO^+ . *J. Chem. Phys.* **81**, 1598.
- Davies, P. B. & Rothwell, W. J. 1984 Diode laser detection of the bending mode of HCO^+ . *J. Chem. Phys.* **81**, 5239.
- Fano, U. 1983 Evolution of quantum defect methods, 1983. *Comments At. Mol. Phys.* **13**, 157.
- Phil. Trans. R. Soc. Lond. A* (1997)

- Foster, S. C. W., McKellar, A. R. & Sears, T. J. 1981 Observation of the ν_3 fundamental band of HCO^+ . *J. Chem. Phys.* **81**, 578.
- Fox, M. A. 1992 Electron transfer: a critical link between subdisciplines in chemistry. *Chem. Rev.* **92**, 365.
- Grant, E. R. 1988 Spectroscopic manifestations of intermediate dynamical processes in optical and ultraviolet multiphoton excitation. In *Advances in multiphoton processes and spectroscopy* (ed. S. H. Lin). Singapore: World Scientific.
- Greene, C. & Jungen, Ch. 1985 Molecular applications of quantum defect theory. *Adv. At. Mol. Phys.* **21**, 51.
- Herzberg, G. & Jungen, Ch. 1972 Rydberg series and ionization potential of the H_2 molecule. *J. Mol. Spectrosc.* **41**, 425.
- Hougen, J. T. 1962 Fermi resonance in linear triatomic molecules in Π electronic states. *J. Chem. Phys.* **37**, 403.
- Jortner, J. & Leach, S. 1980 Perspectives of synchrotron radiation: applications to molecular dynamics and photochemistry. *J. Chem. Phys.* **77**, 7.
- Jortner, J. & Levine, R. D. 1981 Photosensitive chemistry. *Adv. Chem. Phys.* **47**, 1.
- Jungen, Ch. & Atabek, O. 1977 Rovibronic interactions in the photoabsorption spectrum of molecular hydrogen and deuterium, an application of multichannel quantum defect theory methods. *J. Chem. Phys.* **66**, 5584.
- Jungen, Ch. & Dill, D. 1980 Calculation of rotational–vibrational preionization in H_2 by multichannel quantum defect theory. *J. Chem. Phys.* **73**, 3338.
- Jungen, Ch. & Raoult, M. 1981 Spectroscopy in the ionization continuum: vibrational preionization in H_2 calculated by multichannel quantum defect theory, discuss. *Faraday Soc.* **71**, 253.
- Kleinman, V. D., Zhu, I., Li, X. & Gordon, R. J. 1995 Coherent phase control of the photoionization of H_2S . *J. Chem. Phys.* **102**, 5863.
- Kohler, B., Krause, J., Raksi, J. F., Wilson, K. R., Whitnell, R. M., Yakovlev, V. V. & Yan, Y. J. 1995 Controlling the future of matter. *Acc. Chem. Res.* **28**, 133.
- Lucchese, R. R., Takatsuka, K. & McKoy, V. 1986 Applications of the Schwinger variational principle to electron–molecule collisions and molecular photoionization. *Phys. Rep.* **131**, 147.
- Manz, J. & Parmenter, C. S. (eds) 1989 Special issue on mode selectivity in unimolecular reactions. *Chem. Phys.* **139**, 201.
- Matsui, H. & Grant, E. R. 1996 Fermi resonance and mode specificity in the vibrational autoionization of NO_2 . *J. Chem. Phys.* **104**, 42.
- Matsui, H., Mayer, E. E. & Grant, E. R. 1996 Bend-stretch Fermi resonance in NO_2^+ as observed in the two-photon absorption spectroscopy of the $3p\sigma^2\Sigma_u^+$ Rydberg state of NO_2 . *J. Mol. Spectrosc.* **175**, 203.
- Mayer, E. E. & Grant, E. R. 1995 Double-resonance spectroscopy of the high Rydberg states of HCO . I. A precise determination of the adiabatic ionization potential. *J. Chem. Phys.* **103**, 5361.
- Mayer, E. E., Hedderich, H. G. & Grant, E. R. 1997 Consequences of Renner–Teller coupling in the higher vibrational states of the $\text{HCO } 3p\pi^2\Pi$ Rydberg state. (Submitted.)
- McDonald, J. D. 1979 Creation and disposal of vibrational energy in polyatomic molecules. *A. Rev. Phys. Chem.* **30**, 29.
- Miller, W. H. 1987 Tunneling and state specificity in unimolecular reactions. *Chem. Rev.* **87**, 19.
- Park, S. M., Lu, S.-P. & Gordon, R. J. 1991 Coherent laser control of the resonance enhanced multiphoton ionization of HCl . *J. Chem. Phys.* **94**, 8622.
- Pratt, S. T. & Jungen, Ch. 1997 Vibrational autoionization in polyatomic molecules. (In the press.)
- Raoult, M. & Jungen, Ch. 1981 Calculation of vibrational preionization in H_2 by multichannel quantum defect theory. *J. Chem. Phys.* **74**, 3388.
- Ross, S. C. 1991 An MQDT primer. *AIP Conf. Proc.* **225**, 73.
- Phil. Trans. R. Soc. Lond. A* (1997)

- Ross, S. C. & Jungen, Ch. 1994 Multichannel quantum-defect theory of double-minimum $^1\Sigma_g^+$ states in H_2 . II. Vibronic-energy levels. *Phys. Rev. A* **49**, 4364.
- Schinke, R., Keller, H.-M., Stumpf, M. & Dobbyn, A. J. 1995 Vibrational resonances in molecular photodissociation: from state-specific to statistical behaviour. *J. Phys. B* **28**, 3081.
- Schlag, E. W., Müller-Dethlefs, K., Wang, K., McKoy, V. & Grant, E. R. 1995 ZEKE Spectroscopy: high resolution spectroscopy with photoelectrons. *Adv. Chem. Phys.* **90**, 1.
- Shapiro, M. & Brumer, P. 1994 Coherent and incoherent laser control of photochemical reactions. *Int. Rev. Phys. Chem.* **13**, 187.
- Smalley, R. E. 1983 Dynamics of electronically excited states. *A. Rev. Phys. Chem.* **34**, 129.
- Song, X.-M. & Cool, T. A. 1992 Resonance ionization spectroscopy of HCO and DCO. *J. Chem. Phys.* **96**, 8664.
- Stephens, J. A. & Greene, C. H. 1995 Rydberg state dynamics of rotating, vibrating H_3 and the Jahn–Teller effect. *J. Chem. Phys.* **102**, 6946.
- Uzer, T. 1991 Theories of intramolecular vibrational energy transfer. *Phys. Rep.* **199**, 73.
- Warren, W. S., Rabitz, H. & Dahleh, M. 1993 Coherent control of chemical reactions: the dream is alive. *Science* **259**, 1581.
- Yin, Y., Chen, C., Elliott, D. S. & Smith, A. V. 1992 Asymmetric photoelectron angular distributions from interfering photoionization processes. *Phys. Rev. Lett.* **69**, 2353.
- Yin, Y., Chen, C., Elliott, D. S., Shehadeh, R. & Grant, E. R. 1995 Two-pathway coherent control of photoelectron angular distributions in molecular NO. *Chem Phys. Lett.* **241**, 591.

Discussion

C. COSSART-MAGOS (*Laboratoire de Photophysique Moléculaire, Université de Paris-Sud, France*). Professor Grant insisted on mode selectivity in the vibrational autoionization of NO_2 , his experiments showing that symmetric stretching relaxes much faster than the bending motion. In my discussion paper (this volume), I show evidence of similar behaviour in CS_2 . Here, I would like to ask if the very long lifetimes of benzene Rydberg states with $n = 45$ –110 observed in Professor Neusser's group (longer than 1.6 μs , much longer than expected from the lifetimes measured for low- n states, about 500 fs for $n = 5$) would not be in part dependent on the preparation scheme used: UV–UV double resonance involving excitation on the first step of one quantum of the non-totally symmetric vibration $\nu_6(e_{2g})$. It might be too difficult but quite interesting to prepare the same high- n Rydberg states in benzene using a different excitation scheme.

E. R. GRANT. Mode specificity in CS_2 would be very interesting indeed. The Rydberg states sampled by Neusser and co-workers converge to the ground vibrational state of the cation, and thus are not subject to vibrational autoionization. Other things being equal, a change in the vibrational character of the intermediate should not affect final-state dynamics so long as the second step reaches Rydberg series converging to the cation ground-state. Extrapolation of linewidths observed at low- n should be done with care. The very broad lines mentioned in the comment belong to penetrating s-series. Also present in earlier ionization-detected two-photon absorption spectra are much sharper lines which are assigned to d states (Whetten *et al.* 1985).

G. DUXBURY (*Department of Physics and Applied Physics, University of Glasgow, UK*). To what extent does the axis switching between the bent $^2A'$ state of HCO and the linear $3p\pi$ $^2\Pi$ intermediate state of HCO affect the vibrational mode specificity of the autoionization process producing the linear ion HCO^+ ? As the axis switching is different in DCO, does this lead to any different product yield?

E. R. GRANT. In populating long-lived $3p\pi$ Rydberg levels, we prepare what are essentially stationary states with only a laboratory-frame polarization memory of the initial excitation step. The Rydberg–Rydberg transition to autoionizing states is then vertical linear-to-linear, with only the Renner–Teller effect in the $^2\Sigma$ intermediate state to affect intensities, particularly those relating to vibrational angular momentum in the (020) state.

R. J. DONOVAN (*Department of Chemistry, University of Edinburgh, UK*). There is an important and interesting difference between NO_2 and HCO in that the former will have low-lying ion-pair states, due to the low ionization energy of NO and the substantial electron affinity of O. For HCO both H and CO have high ionization energies and their electron affinities are small. The ion-pair states of HCO will thus lie at high energy. Does Professor Grant see any evidence for the involvement of ion-pair states in the Rydberg spectroscopy of NO_2 ?

E. R. GRANT. The issue of ion-pair states is an important one. The thermochemical limit for forming $\text{NO}^+ + \text{O}^-$ lies only 1.3 eV above the adiabatic ionization threshold of NO_2 . It would be nice to have calculations detailing the multidimensional exit channel for ion-pair formation to compare with the NO_2^+ potentials of the Rydberg cores.

Additional references

Whetten, R. L., Grubb, S., Otis, C. E., Albrecht, A. C. & Grant, E. R. 1985 Higher excited states of benzene: polarized ultraviolet two-photon absorption spectroscopy. *Chem. Phys.* **82**, 115.

MATHEMATICAL,
PHYSICAL
& ENGINEERING
SCIENCES

THE ROYAL
SOCIETY

PHILOSOPHICAL
TRANSACTIONS
OF

MATHEMATICAL,
PHYSICAL
& ENGINEERING
SCIENCES

THE ROYAL
SOCIETY

PHILOSOPHICAL
TRANSACTIONS
OF